Organic & Biomolecular Chemistry

Cite this: *Org. Biomol. Chem.*, 2012, **10**, 2413

www.rsc.org/obc

PAPER

Novel peptide foldameric motifs: a step forward in our understanding of the fully-extended conformation/3_{10}-helix coexistence†‡

Fernando Formaggio,*[a] Marco Crisma,[a] Gema Ballano,[a] Cristina Peggion,[a] Mariano Venanzi[b] and Claudio Toniolo*[a]

Received 4th November 2011, Accepted 2nd February 2012
DOI: 10.1039/c2ob06863j

The fully-extended, multiple C_5, conformation or 2.0_5 helix is a very appealing peptide secondary structure, in particular for its potential use as a molecular spacer, as it is characterized by the longest elevation (as high as 3.62 Å) between the α-carbon atoms of two consecutive α-amino acids. Despite this intriguing property, however, it is only poorly investigated and understood. Here, using a complete series of $C^{\alpha,\alpha}$-diethylglycine (Deg) homo-oligopeptide esters to the pentamer level, we exploited the properties of a fluorophore and a quencher, synthetically positioned at the N- and C-termini of the main chain, respectively, to check the applicability of the fully-extended conformation as a rigid molecular spacer. The fluorescence study was complemented by FT-IR absorption and NMR conformational investigations. The X-ray diffraction structures of selected compounds are also reported. Unfortunately, we find that, even in a solvent of low polarity, such as chloroform, in this peptide series an equilibrium does take place between the fragile fully-extended conformation and the 3_{10}-helical structure, the latter becoming more and more stable as the main chain is elongated. Since the Deg homo-peptide esters lacking any terminal aromatic group, previously investigated, are known to adopt a stable fully-extended conformation in chloroform solution, we tend to attribute the 3D-structure instability observed in this work to the presence of multiple aromatic rings in their blocking groups.

Introduction

The incorporation of $C^{\alpha,\alpha}$-dialkylated glycyl residues into peptide chains provides a mean for efficiently restricting the ϕ,ψ backbone conformational space. A wealth of information from solution and crystal-state studies and conformational energy computations as well clearly demonstrated that $C^{\alpha,\alpha}$-dimethylglycine (or α-aminoisobutyric acid, Aib), shown in Fig. 1, strongly stabilizes 3_{10}- and α-helical structures.[1–3] In contrast, works from our laboratory and other groups (in particular that of Tanaka/Suemune)[4–19] showed that either the 3_{10}-helix[20] or, interestingly, a novel polypeptide 3D-structure termed fully-extended conformation or 2.0_5-helix[8] is preferentially adopted by homo-peptides from $C^{\alpha,\alpha}$-diethylglycine (Deg; Fig. 1). Since this latter peptide 3D-structure appears to be rather fragile, we are currently investigating the most appropriate chemical (*e.g.*, effect of terminal groups)[21] and environmental (*e.g.*, effect of nature of solvent)[22] conditions to increase its stability.

The repeating motif of the 2.0_5-helix is the N_i–H_i ···O_i=C_i' intramolecularly H-bonded C_5 conformation,[23,24] shown in Fig. 1 along with its 3D-structural parameters. The relative disposition of the two dipoles, N_i–H_i and C_i'=O_i, is such that there is obviously some interaction between them. Since these four atoms, together with the C_i^{α} atom, are involved in a pentagonal "pseudo" cyclic structure, this conformation is also called the C_5 structure.

In view of its relevant interest as a molecular spacer, the goal of our present work was to exploit the fully-extended peptide secondary structure in a fluorescence study. Indeed, the elevation per residue of this flat helix is the longest (as high as 3.62 Å) among those of peptide 3D-structures.[8] To this end, we incorporated an 1-pyrenylacetyl (PyrAc) group (Fig. 1) at the backbone N-terminus as the fluorophore, and a *para*-nitrobenzoxy [*O*-(pNO$_2$)Bzl] group at the C-terminus as the quencher.[25,26]

[a]*ICB, Padova Unit, CNR, Department of Chemistry, University of Padova, 35131 Padova, Italy. E-mail: fernando.formaggio@unipd.it, claudio.toniolo@unipd.it; Fax: +39-049-8275829; Tel: +39-049-8275247*
[b]*Department of Chemical Sciences and Technologies, University of Rome "Tor Vergata", 00133 Rome, Italy*

† This article is part of an *Organic & Biomolecular Chemistry* web theme issue on Foldamer Chemistry.

‡ Electronic supplementary information (ESI) available: Tables of selected torsion angles and H-bond parameters, and packing figures for the X-ray diffraction structures of PyrAc-(Deg)$_2$-*O*-(pNO$_2$)Bzl, PyrAc-(Deg)$_5$-*O*-(pNO$_2$)Bzl, and PyrAc-(Aib)$_5$-O*t*Bu. CCDC 846155–846157. For ESI and crystallographic data in CIF or other electronic format see DOI: 10.1039/c2ob06863j

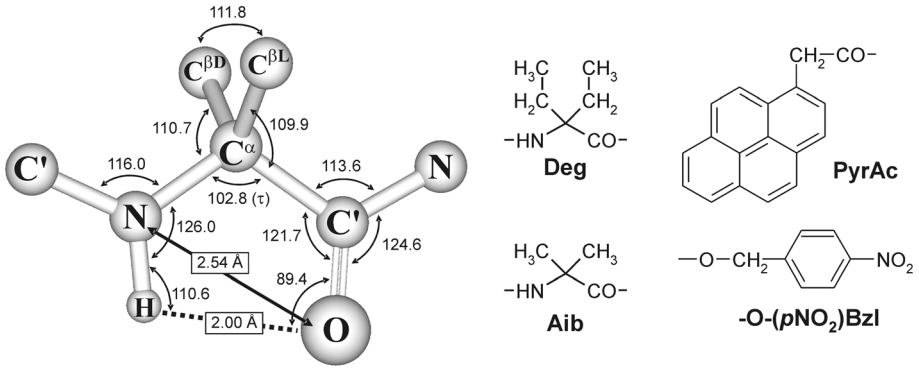

Fig. 1 (A) Average geometrical parameters for the fully-extended, intramolecularly H-bonded, C_5 conformation from a statistical analysis of X-ray diffraction structures.[8] In addition, the chemical formulas of Deg, Aib, PyrAc, and *O*-(*p*NO_2)Bzl are shown.

Results and discussion

Peptide synthesis and characterization

The N^{α}-protected Deg derivatives Tfa-Deg-OH (Tfa, trifluoroacetyl),[27] Z-Deg-OH (Z, benzyloxycarbonyl),[27,28] and Z-Deg-O*t*Bu (O*t*Bu, *tert*-butoxy)[29] are known compounds. The synthesis and characterization of the homo-peptides Tfa-(Deg)$_n$-O*t*Bu (n = 2–5) were also reported.[27,28]

Our strategy for the preparation of the PyrAc-(Deg)$_n$-*O*-(*p*NO_2)Bzl (n = 1–5) peptides first involves the introduction of the PyrAc moiety in the N^{α}-deprotected H-(Deg)$_n$-O*t*Bu peptides (obtained, in turn, by Tfa removal of the corresponding N^{α}-Tfa protected oligomers with $NaBH_4$ in ethanol)[12,27] using the 1-(3-dimethylamino)propyl-3-ethylcarbodiimide/7-aza-1,2,3-benzotriazole method[30,31] in anhydrous acetonitrile. The PyrAc-protected peptide free acids, PyrAc-(Deg)$_n$-OH, were prepared by dissolving the corresponding *tert*-butyl esters in a 6 : 4 trifluoroacetic acid–dichloromethane mixture. In the last step, the target PyrAc-(Deg)$_n$-*O*-(*p*NO_2)Bzl peptides were synthesized from the corresponding free acids and *para*-nitrobenzylbromide in the presence of triethylamine and silver oxide in acetone or in a 95 : 5 acetonitrile–water mixture.

Finally, the two control compounds PyrAc-(Aib)$_5$-*O*-(*p*NO_2)Bzl and Ac-*O*-(*p*NO_2)Bzl (Ac, acetyl) were synthesized as described above for the PyrAc-(Deg)$_n$-*O*-(*p*NO_2)Bzl peptides starting from Z-(Aib)$_5$-O*t*Bu[32,33] and Ac–OH, respectively.

The final peptides and their synthetic intermediates, all of them of high chromatographic purity, were characterized by melting point determination (where appropriate), thin-layer chromatography (TLC) in three solvent systems, solid-state IR absorption, and ^{1}H NMR data. In addition, electrospray ionization mass spectra (ESI-MS) were collected for all of the –*O*-(*p*NO_2)Bzl ester peptides.

Conformational analysis in the crystal state

We were able to grow single crystals useful for X-ray diffraction investigations from three of the PyrAc-containing peptides synthesized in this work. They are: PyrAc-(Deg)$_n$-*O*-(*p*NO_2)Bzl (n = 2 and 5) and PyrAc-(Aib)$_5$-O*t*Bu (Fig. 2–4, respectively). Lists of the most significant conformational and H-bond parameters are reported in the ESI (Tables S1 to S6‡).

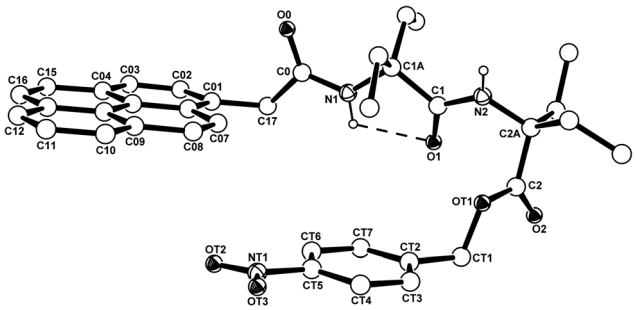

Fig. 2 X-Ray diffraction structure of PyrAc-(Deg)$_2$-*O*-(*p*NO_2)Bzl with partial atom numbering. Only the major occupancy sites for the atoms belonging to the disordered PyrAc moiety are shown. The intramolecular H-bond is represented by a dashed line.

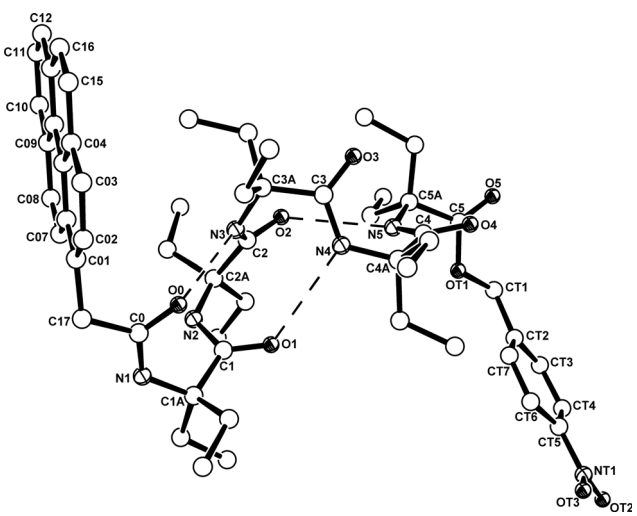

Fig. 3 X-Ray diffraction structure of PyrAc-(Deg)$_5$-*O*-(*p*NO_2)Bzl with partial atom numbering. The three intramolecular H-bonds are represented by dashed lines.

In the three peptides, only one τ (N–C^{α}–C′) bond angle[8,34] [104.22(11)°] is well below 109.5°, the value expected for a regular tetrahedral sp^3 carbon atom. This angle pertains to residue 1 of the Deg dipeptide. This property is typically taken as a preliminary evidence for the occurrence of the strain

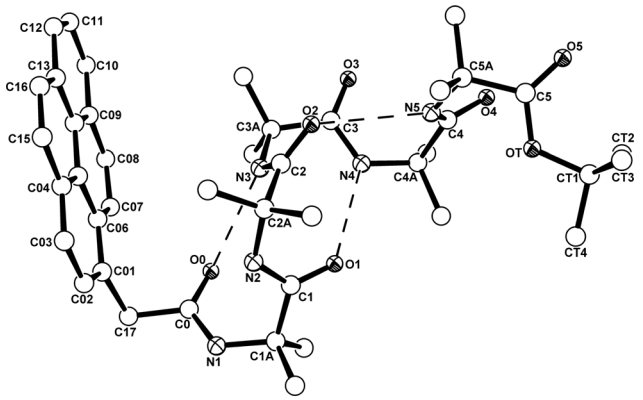

Fig. 4 X-Ray diffraction structure of PyrAc-(Aib)$_5$-O*t*Bu with partial atom numbering. The three intramolecular H-bonds are represented by dashed lines.

characterizing the intramolecularly H-bonded C_5(pentagonal)-pseudoring conformation.[8]

In the Deg homo-dipeptide crystal structure (Fig. 2) residue 1 shows values for the backbone torsion angles close to 180°, 180° [$\phi_1 = \pm171.3(1)°$, $\psi_1 = \pm169.5(1)°$, since molecules of both handedness simultaneously occur in its centrosymmetric space group, $P2_1/n$] indicative of the fully-extended C_5 conformation.[8] The intramolecular N1···O1 distance is 2.567(2) Å. However, the second residue is folded in a helical conformation, with $\phi_2 = \pm43.0(2)°$, "ψ_2" = ±45.3(2)°.

The Deg homo-pentapeptide, although not containing any asymmetric carbon atom, crystallizes in a non-centrosymmetric space group ($P2_1$). As a consequence, only molecules of the same handedness occur in each crystal. This is a rather uncommon phenomenon, termed *spontaneous resolution*.[35,36] We assigned the right-handed enantiomorph to the crystal selected for the analysis since the value of the Flack parameter[37,38] [0.0 (2)] indicates that it is the most probable one. Nevertheless, in the absence of strong anomalous scatterers, this choice does not imply that we have determined the absolute configuration of the helical molecular species of the Deg homo-pentapeptide. In the crystal structure (Fig. 3), the peptide backbone adopts a 3_{10}-helical conformation generated by three consecutive, intramolecularly H-bonded, C_{10} forms. The set of backbone torsion angles is $\phi_1 = -53.8(3)°$, $\psi_1 = -41.7(3)°$; $\phi_2 = -55.0(4)°$, $\psi_2 = -31.5(3)°$; $\phi_3 = -53.4(3)°$, $\psi_3 = -34.8(3)°$; $\phi_4 = -59.2(3)°$, $\psi_4 = -31.5(3)°$; $\phi_5 = 49.9(3)°$, "ψ_5" = 54.8(3)°. The range of N···O distances is normal, 2.862(3) Å–3.218(3) Å,[39] as it is that of the N–H···O angles: 143°–174°. For all five helical Deg residues the value of the τ bond angle is between 109.8(2)° and 112.0(2)°.

As expected for an Aib homo-peptide,[2,3] in the crystal structure of PyrAc-(Aib)$_5$-O*t*Bu the molecules are folded in a 3_{10}-helical structure (Fig. 4) with three C═O···H–N intramolecular H-bonds. In this case, the achiral molecules crystallize normally in a centrosymmetric space group ($P\bar{1}$). The set of backbone torsion angles is: $\phi_1 = \pm55.4(2)°$, $\psi_1 = \pm31.4(2)°$; $\phi_2 = \pm55.0(2)°$, $\psi_2 = \pm30.4(2)°$; $\phi_3 = \pm52.2(2)°$, $\psi_3 = \pm35.8(2)°$; $\phi_4 = \pm57.9(2)°$, $\psi_4 = \pm37.6(2)°$; $\phi_5 = -/+49.3(2)°$, "ψ_5" = −/+43.2 (2)°. The range of the intramolecular H-bonding N···O separations is 2.921(1)–3.141(1) Å and that of the N–H···O angles is 150°–162°. The range of the τ bond angles for the five Aib residues is 109.9(1)°–111.1(1)°. Overall, the molecular conformations of the Deg and Aib homo-pentapeptides in the crystal state are quite similar.

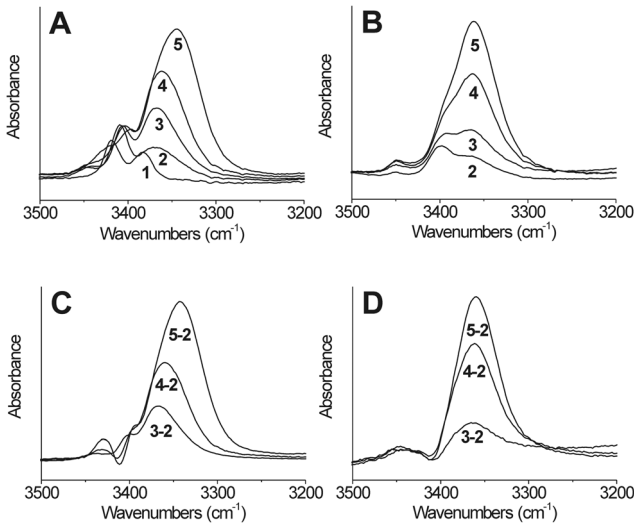

Fig. 5 FT-IR absorption spectra in the 3500–3200 cm^{-1} region of (A) PyrAc-(Deg)$_n$-*O*-(*p*NO$_2$)Bzl (n = 1–5) and (B) PyrAc-(Deg)$_n$-O*t*Bu (n = 2–5). Spectra obtained by subtracting that of PyrAc-(Deg)$_2$-*O*-(*p*NO$_2$)Bzl from those of PyrAc-(Deg)$_n$-*O*-(*p*NO$_2$)Bzl (n = 3–5) (C), and that of PyrAc-(Deg)$_2$-O*t*Bu from those of PyrAc-(Deg)$_n$-O*t*Bu (n = 3–5) (D) are also shown. Peptide concentration ($CDCl_3$): 1 mM.

The crystallographic results reported in this work, together with those reported in the literature,[2,3,5,7–9,12] strongly suggest that the $C^{\alpha,\alpha}$-diethylated Deg residue can adopt either the fully-extended C_5 conformation or the helical structure under these conditions, whereas the $C^{\alpha,\alpha}$-dimethylated Aib residue overwhelmingly prefers to fold in a helix. Indeed, the homo-pentapeptide Tfa-(Deg)$_5$-O*t*Bu is 2.0$_5$-helical (fully-extended) in the crystal state,[5] but the 3D-structures of Tfa-(Deg)$_5$-OEt (OEt, ethoxy)[12] and PyrAc-(Deg)$_5$-*O*-(*p*NO$_2$)Bzl, the latter described here, are 3_{10}-helical. It remains to be seen whether crystal packing, in particular originated from different crystallization solvents and/or different blocking (protecting) groups, has played any role in governing peptide conformation in Deg homo-peptides. For example, in our PyrAc-/-*O*-(*p*NO$_2$)Bzl homo-di and pentapeptides, dyads of pyrenyl and *para*-nitrophenyl moieties of *different* molecules, separated by an intermolecular distance of 3.5 Å, interact each other *via* π···π stacking (Fig. S1 and S2 in the ESI‡).

Conformational analysis in chloroform solution

The conformational preferences of the PyrAc/*O*-(*p*NO$_2$)Bzl blocked Deg homo-peptides to the pentamer level were examined in $CDCl_3$, a solvent of low polarity, by use of FT-IR absorption and ^{1}H NMR.

Keeping in mind the IR absorption properties in the amide A region of the Tfa/O*t*Bu protected, fully-extended (Deg)$_n$ peptides[6] and the 3_{10}-helical (Aib)$_n$ homo-peptides,[40] we analyzed the spectra of the PyrAc-(Deg)$_n$-*O*-(*p*NO$_2$)Bzl (n = 1–5) peptides (Fig. 5A and C). In particular, the difference spectra of the shortest peptides reveal a strong band at about 3360 cm^{-1}

and a very weak band near 3440 cm^{-1}, characteristic of the C_5 conformation.[6,23] However, the strong band moves to lower frequencies for the longest oligomers, as expected for 3_{10}-helical peptides.[40] More specifically, the band of the homo-pentamer attributed to intramolecularly H-bonded conformers appears at 3340 cm^{-1}, close to that of the 3_{10}-helical PyrAc-$(Aib)_5$-*O*-(pNO_2)Bzl (3344 cm^{-1}) (not shown). In conclusion, our view is that the conformational equilibrium mixtures of PyrAc/*O*-(pNO_2)Bzl Deg homo-peptides tend to evolve from the multiple C_5 conformation to the predominant 3_{10}-helix as the peptide length is enhanced from the homo-trimer to the pentamer.

Furthermore, we checked the role of the terminal groups on peptide conformation. In the spectrum of the tetrapeptide Tfa-$(Deg)_4$-*O*-(pNO_2)Bzl (not shown), three bands are seen: 3448 cm^{-1} (very weak), 3406 cm^{-1} (weak), and at about 3360 cm^{-1} (intense and broad). Overall, the spectrum is reasonably close to that of a peptide in the fully-extended conformation. Also, the spectra, and the difference spectra as well, of the PyrAc-$(Deg)_n$-O*t*Bu (n = 2–5) peptide series (Fig. 5B and D) resemble those of fully-extended peptides (in particular, the occurrence of a very weak band at 3447–3450 cm^{-1} and a main band at 3360 cm^{-1} in the difference spectra is significant). From these data, we tend to conclude that it is the combination of the two large aromatic moieties [PyrAc and (pNO_2)Bzl] that is somewhat deleterious to the stabilization of the fully-extended conformation in the Deg homo-peptides.

We also expanded our FT-IR absorption analysis to the 1750–1450 cm^{-1} region. Typically, 3_{10}-helical oligopeptides exhibit a strong band near 1665 cm^{-1} (amide I), followed by a less intense band at approximately 1515 cm^{-1} (amide II).[41] In the shortest peptides, this latter absorption occurs as two bands (free and H-bonded N–H groups, respectively), with that of H-bonded N-Hs prevailing for longer peptides. The band above 1700 cm^{-1} is assigned to the C═O stretching mode of the ester chromophore. In contrast, in the case of the fully-extended peptides Tfa-$(Deg)_n$-O*t*Bu (n = 2–5) the amide II band is significantly more intense than that of the amide I (Fig. 6A). This latter band is seen at about 1665 cm^{-1} as a double peak with a separation as large as 25 cm^{-1} for the pentapeptide. The amide II signal appears as a single band, which is shifted to lower wavenumbers as compared to that of 3_{10}-helical peptides and moves further down as the peptide chain is elongated.

The spectral behavior of the PyrAc/*O*-(pNO_2)Bzl blocked Deg homo-oligomers is somewhat intermediate between those of the 3_{10}-helical and fully-extended peptides. In particular, in the difference spectra (Fig. 6B) the amide I absorption shows a double peak typical of the latter conformation, but the absorption of the pentapeptide resembles more that of the $(Aib)_5$ homo-oligomer (also shown in Fig. 6B). Also in the amide II region (at least above 1500 cm^{-1}) there is a tendency for the spectrum of the $(Deg)_5$ peptide to approach that of $(Aib)_5$. Further information was obtained from observation of the spectra of Tfa-$(Deg)_4$-*O*-(pNO_2)Bzl (Fig. 6C) and the difference spectra of the PyrAc-$(Deg)_n$-O*t*Bu (n = 3–5) (Fig. 6D), which are all quite close to that expected for peptides in the fully-extended conformation. To summarize, our solution conformational analysis based on the amide I/II regions of the FT-IR absorption spectra of the peptides examined nicely confirm the conclusions presented above from the amide A data.

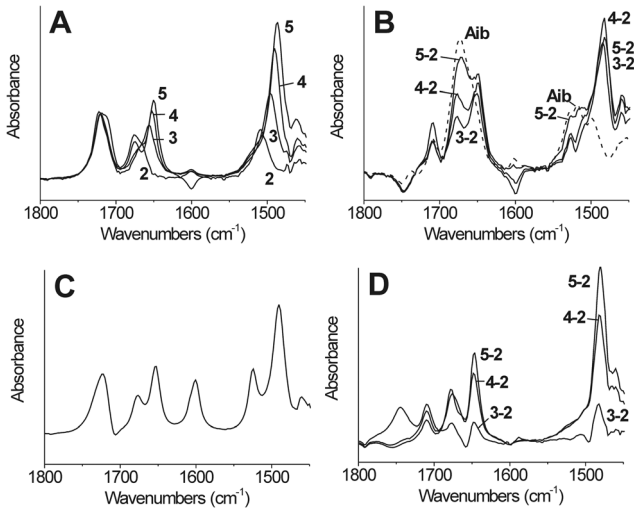

Fig. 6 FT-IR absorption spectra in the 1750–1450 cm^{-1} region of: (A) Tfa-$(Deg)_n$-O*t*Bu (n = 2–5), (B) PyrAc-$(Deg)_n$-*O*-(pNO_2)Bzl (n = 3–5) [these are difference spectra obtained by subtracting that of PyrAc-$(Deg)_2$-*O*-(pNO_2)Bzl from those of its higher homologs] and PyrAc-$(Aib)_5$-*O*-(pNO_2)Bzl (Aib), (C) Tfa-$(Deg)_4$-*O*-(pNO_2)Bzl, and (D) PyrAc-$(Deg)_n$-O*t*Bu (n = 3–5) [these are difference spectra obtained by subtracting that of PyrAc-$(Deg)_2$-O*t*Bu from those of its higher homologs]. Peptide concentration ($CDCl_3$): 1 mM.

Additional information on the secondary 3D-structural propensities of the PyrAc/*O*-(pNO_2)Bzl blocked Deg homo-oligopeptides were extracted from an NMR investigation. Typical titrations in $CDCl_3$ solution as a function of addition of the strong H-bonding acceptor solvent dimethylsulfoxide (DMSO):[42–44] (i) For the 3_{10}-helix forming $(Aib)_5$ homo-peptide (Fig. 7A), they induce a shift to higher δ values only for the N-terminal NH(1) and NH(2) protons (much more pronounced for the former), not intramolecularly H-bonded with any C═O group of the peptide. (ii) For the fully-extended Tfa-$(Deg)_4$-O*t*Bu peptide (Fig. 7 B and ref. 6), they do not produce any sizable shift in the signals of the four NH protons, which suggests that these protons are solvent protected. In addition, the close positions of all four NH proton signals at low field (above 7.0 ppm), similar to those of the three C-terminal NH proton signals of $(Aib)_5$, definitely confirm their participation in H-bonds. When the C-terminal alkyl ester (O*t*Bu) is replaced by an arylalkyl ester, as in Tfa-$(Deg)_4$-*O*-(pNO_2)Bzl, only one NH proton chemical shift becomes sensitive (moving to higher δ values) to the addition of DMSO (Fig. 7C). We assign this signal to the NH(4) proton, near the aromatic, C-terminal protecting group (which also produces a downfield shift by about 0.30 ppm in the position of this proton in $CDCl_3$ as compared to that of the corresponding proton in the O*t*Bu ester). Finally, the $CDCl_3$–DMSO titration curve for the PyrAc/*O*-(pNO_2)Bzl Deg homo-tetramer (Fig. 7D) is clearly anomalous and difficult to interpret, in the sense that it is quite distinct from those characteristic of either the fully-extended or the 3_{10}-helical peptides. In the curve of this tetrapeptide, all NH proton chemical shifts move somewhat (0.30–0.70 ppm) from their original positions in $CDCl_3$. Two of them, NH(1) and NH(4), are downfield shifted, whereas the other two, NH(3) and particularly NH(2), are unusually *upfield* shifted. Furthermore, the signals of all these NH protons

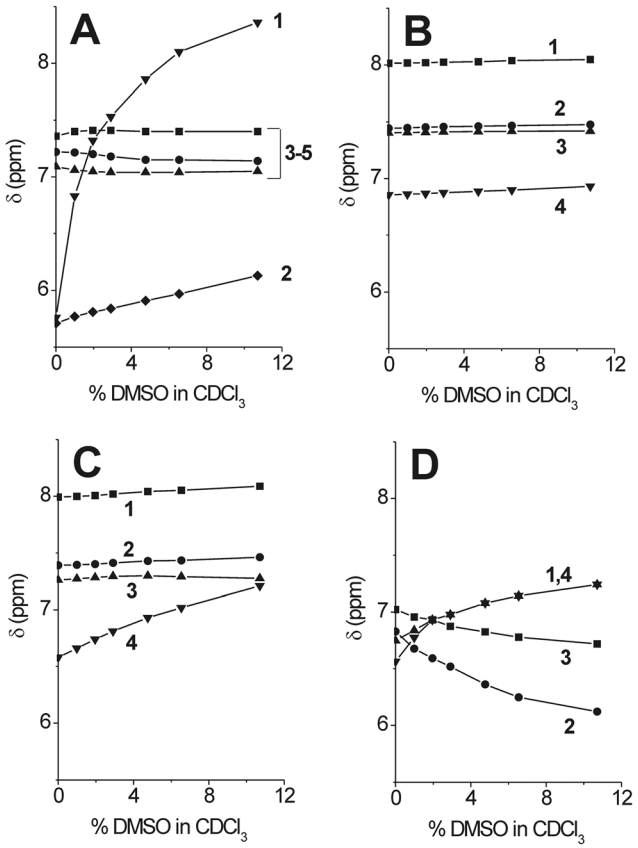

Fig. 7 Plots of the NH proton chemical shifts in the ^{1}H NMR spectra of (A) PyrAc-(Aib)$_5$-*O*-(*p*NO$_2$)Bzl, (B) Tfa-(Deg)$_4$-O*t*Bu, (C) Tfa-(Deg)$_4$-*O*-(*p*NO$_2$)Bzl, and (D) PyrAc-(Deg)$_4$-*O*-(*p*NO$_2$)Bzl as a function of increasing percentages of DMSO added to the CDCl$_3$ solution (v/v) (peptide concentration: 1 mM).

tend to broaden as DMSO is added, which might indicate the concomitant occurrence of multiple conformers in the solution equilibrium mixture. Taken together, these NMR results reinforce our conclusion that the PyrAc/*O*-(*p*NO$_2$)Bzl system is not an appropriate choice for the stabilization of a fully-extended structure in Deg homo-peptides.

Molecular spacers

We checked the applicability of the PyrAc-(Deg)$_n$-*O*-(*p*NO$_2$)Bzl peptides as fully-extended molecular spacers in a static fluorescence study. To perform a very stringent comparison with our IR absorption and NMR results, the solvent used was chloroform, despite the fact that in principle it would not be the best choice for a fluorescence analysis, due to the presence, although to a limited extent, of potentially quenching chlorine atoms in solution. The spectra were recorded after excitation of the samples at 346 nm, where the pyrenyl chromophore is known to exhibit its strongest absorption (related to a symmetry allowed $\pi \rightarrow \pi^*$ transition) above 300 nm.[25,26]

In the fluorescence spectra above 350 nm, the pyrenyl chromophore is characterized by two main bands located near 375 nm and 395 nm endowed with fine structure.[25,26] A simple visual inspection of the curves, shown in Fig. 8 in comparison with that of the blank (PyrAc-OH), which lacks any quencher

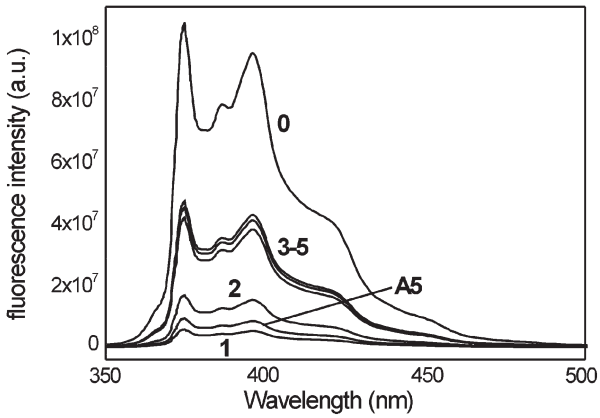

Fig. 8 Fluorescence spectra of the blank PyrAc–OH (0), the Deg derivative and peptides PyrAc-(Deg)$_n$-*O*-(*p*NO$_2$)Bzl (n = 1–5) (1–5), and the Aib peptide PyrAc-(Aib)$_5$-*O*-(*p*NO$_2$)Bzl (A5) in CHCl$_3$ solution (concentration: 10^{-7} M).

group in its molecule, reveals that: (i) No pyrene excimer emission band is seen. (ii) The trend in quenching efficiency for the shortest members of the series, the (Deg)$_{1-3}$ peptides, steadily decreases from 0.97 (n = 1) to 0.89 (n = 2), and 0.64 (n = 3). This finding is compatible with the conclusion that these three peptides are all essentially fully-extended in CHCl$_3$ solution. However, the quenching efficiencies for our longest Deg homo-peptides, 0.68 for n = 4 and 0.65 for n = 5, are not further reduced. The inevitable conclusion is that the tetra- and penta-peptides populate at least two different conformations, where the probe dyads are located at different relative distances. Unfortunately, this preliminary fluorescence investigation does not allow us to assign the relative populations to each of the secondary structures attained by these two oligomers. In any case, a reasonable view is that in CHCl$_3$ the (Deg)$_4$ and (Deg)$_5$ peptides tend to adopt mixtures of fully-extended and 3$_{10}$-helical conformers, with the amount of the latter increasing from the tetra- to the pentamer level. Notably, these results fit well with those obtained from our IR absorption and NMR studies in the same solvent of low polarity.

We obtained further interesting information from the fluorescence spectrum of the 3$_{10}$-helical pentamer PyrAc-(Aib)$_5$-*O*-(*p*NO$_2$)Bzl, also reported in Fig. 8. This relatively long oligomer is quenched more than (Deg)$_2$, but slightly less than the Deg monomer (quenching efficiency: 0.94). In particular, these findings clearly indicate that the shortest distance for the fluorophore–quencher dyad experienced by the Aib pentamer molecule is more reduced than that occurring in the Deg dimer (and much more reduced than that present in the related Deg pentamer). It is worth pointing out that in this phenomenon a significant role could be played not only by the peptide backbone solution conformations, but by the rotamers around the two single bonds characterizing each of the probes as well, not necessarily correctly represented by those experimentally found in the crystal state for the (Deg)$_2$ and (Deg)$_5$ peptides (Fig. 2–4).

Conclusions

The fully-extended conformation is by far the most stretched per residue peptide 3D-structure. In this specific rank order it is

followed by the β-sheet conformation, and the type-II poly-(Pro)$_n$, 3_{10}- and α-helices. So far, this potentially quite useful property of the fully-extended conformation has not been exploited at all because: (i) This 3D-structure is constitutionally fragile.[21,22] (ii) The synthesis of homo-peptides typically adopting it is difficult and the coupling yields usually obtained are not amenable to the solid-phase methodology.[45]

The classical α-amino acid residue recommended for building up this unusual peptide secondary structure is Deg.[4–19] We and others have already shown that the most stabilizing, terminal protecting (or blocking), groups of the peptide main-chain, at least in chloroform solution, are Tfa at the N-terminus and an alkyl ester at the C-terminus.[5,6,12] In the Tfa-protected Deg homo-peptides, the N-terminal residue is held tightly in the C_5 conformation by virtue of a stabilizing, multiple H-bonding of the F···H(N$_1$)···O$_1$=C$_1$ type. A C-terminal primary or secondary amide is not tolerated because its unsatisfied –NH– function can provide the H-bonding donor responsible for the switch of this extremely elongated 3D-structure to the more compressed 3_{10}-helix.[21] Also, to avoid destabilization of the fully-extended conformation, the solvent of choice is chloroform. Intermolecular H-bonds arising from solvents of higher polarity[22] and packing forces occurring in crystals[12] may compete with the weak intraresidue H-bond of the C_5 basic unit, thus switching the conformation to the 3_{10}-helix.

In this work, we made an attempt to exploit the fully-extended peptide conformation as a rigid molecular ruler using (static) fluorescence spectroscopy. However, this physico-chemical technique implies the introduction of aromatic moieties as a fluorophore and a quencher. The results of our present combination of FT-IR absorption, NMR, and X-ray diffraction techniques force us to conclude that not only in the crystal state, but in chloroform as well, in the Deg homo-peptides investigated the fully-extended conformation and the 3_{10}-helix coexist to different extents. Clearly, terminal aromatic groups are not eligible for the fabrication of a stable fully-extended conformation, at least in this homo-peptide series.

We are currently extending our investigation of this conformation in Deg homo-peptides in chloroform solution to an NMR-based technique, REDOR,[46] which allows the use of the fluorine atoms of the stabilizing Tfa group at the N-terminus as a first probe and requires an appropriate isotopically labelled Deg residue or protecting group at the C-terminus as the second probe.

Experimental

Peptide synthesis and characterization

General methods. Melting points were determined in capillary tubes by use of a Stuart SMP10 apparatus (Bibby Scientific, Stone, Staffordshire, UK) and are uncorrected. ESI-MS were obtained by using a PerSeptive Biosystem Mariner model instrument (Framingham, MA). Flash chromatography was carried out by use of a Merck (Darmstadt, Germany) silica gel 60 (40–63 μm mesh) stationary phase. Analytical TLC was performed on Kieselgel F 254 precoated plates (Merck). The retention factors (R_f) values were determined using the following solvent mixtures as eluants: R_f1 chloroform–ethanol 9 : 1; R_f2 1-butanol–acetic acid–water 3 : 1 : 1; R_f3 toluene–ethanol 7 : 1. The chromatograms were visualized by UV fluorescence or developed by chlorine–starch–potassium iodide or ninhydrin chromatic reaction as appropriate. All compounds were obtained in a chromatographically homogeneous state. The solid-state IR absorption spectra (KBr disk technique) were recorded with a Perkin-Elmer model 1720X FT-IR spectrophotometer.

PyrAc-Deg-O*t*Bu. This compound was obtained from PyrAc-OH (Aldrich, St. Louis, MO) and H-Deg-O*t*Bu (the latter prepared in turn by catalytic hydrogenation of Z-Deg-O*t*Bu in anhydrous CH_2Cl_2) in anhydrous CH_3CN in the presence of EDC–HOAt. Yield: 21%. Melting point: oil. TLC R_f1: 0.95; R_f2: 0.95; R_f3: 0.85. ^{1}H NMR (200 MHz; $CDCl_3$): δ 8.36 (d, 1H, Pyr CH), 8.14–7.93 (m, 8H, 8 Pyr CH), 6.40 (s, 1H, NH), 4.29 (s, 2H, PyrAc CH_2), 2.43 (m, 2H, Deg β-CH_2), 1.60 (m, 2H, Deg β-CH_2), 1.28 (s, 9H, O*t*Bu CH_3), 0.59 (t, 6H, Deg γ-CH_3).

PyrAc-Deg-OH. This compound was prepared from PyrAc-Deg-O*t*Bu by treatment with TFA diluted with CH_2Cl_2. Yield: 95%. Melting point: 279–281 °C [after repeated washings with diethyl ether (Et_2O)]. TLC R_f1: 0.25; R_f2: 0.95; R_f3: 0.35. ^{1}H NMR (400 MHz; DMSO, d_6): δ 8.42–7.98 (m, 9H, Pyr CH), 7.79 (s, 1H, NH), 4.28 (s, 2H, PyrAc CH_2), 1.98 (m, 2H, Deg β-CH_2), 1.74 (m, 2H, Deg β-CH_2), 0.68 (t, 6H, Deg γ-CH_3).

PyrAc-Deg-*O*-(*p*NO$_2$)Bzl. This compound was prepared from PyrAc-Deg-OH and 4-nitrobenzylbromide in acetone solution in the presence of triethylamine and Ag_2O. Yield: 34%. Melting point: 141–143 °C [from CH_2Cl_2–petroleum ether (PE)]. TLC R_f1: 0.95; R_f2: 0.95; R_f3: 0.70. IR (KBr): 3385, 1738, 1649, 1519 cm^{-1}. ^{1}H NMR (400 MHz; $CDCl_3$): δ 8.27–7.92 (m, 11H, 9 Pyr and 2 Bzl CH), 7.18 (d, 2H, 2 Bzl CH), 6.10 (s, 1H, NH), 5.00 (d, 2H, Bzl CH_2), 4.30 (s, 2H, PyrAc CH_2), 2.30 (m, 2H, Deg β-CH_2), 1.75 (m, 2H, Deg β-CH_2), 0.53 (m, 6H, Deg γ-CH_3). MS (ESI-TOF): $[M + H]^+_{calcd}$ 509.213; $[M + H]^+_{exptl}$ 509.212.

PyrAc-(Deg)$_2$-O*t*Bu. This compound was prepared from PyrAc-OH and H-(Deg)$_2$-O*t*Bu [the latter obtained in turn from $NaBH_4$ treatment of Tfa-(Deg)$_2$-O*t*Bu[27,28] in ethanol under reflux] in anhydrous CH_3CN in the presence of EDC–HOAt. Yield: 21%. Melting point: 131–133 °C [from ethyl acetate (EtOAc)–PE]. TLC R_f1: 0.95; R_f2: 0.95; R_f3: 0.70. IR (KBr): 3399, 3341, 1721, 1653, 1494 cm^{-1}. ^{1}H NMR (400 MHz; $CDCl_3$): δ 8.27 (d, 1H, 1 Pyr CH), 8.10–7.86 (m, 8H, 8 Pyr CH), 6.82 (s, 1H, NH^1), 6.61 (s, 1H, NH^2), 4.29 (s, 2H, PyrAc CH_2), 2.45 (m, 2H, Deg^1 β-CH_2), 2.20 (m, 2H, Deg^2 β-CH_2), 1.60 (m, 4H, Deg β-CH_2), 1.32 (s, 9H, O*t*Bu CH_3), 0.56 (m, 12H, Deg γ-CH_3).

PyrAc-(Deg)$_2$-OH. This compound was prepared from PyrAc-(Deg)$_2$-O*t*Bu as described above for PyrAc-Deg-OH. Yield: 94%. Melting point: 223–225 °C (after repeated washings with Et_2O). TLC R_f1: 0.25; R_f2: 0.95; R_f3: 0.30. ^{1}H NMR (400 MHz; DMSO, d_6): δ 8.7–8.03 (m, 9H, 9 Pyr CH), 7.77 (s, 1H, NH), 7.32 (s, 1H, NH), 4.29 (s, 2H, PyrAc CH_2), 2.09 (m, 2H, Deg β-CH_2), 1.85 (m, 4H, Deg β-CH_2), 1.67 (m, 2H, Deg β-CH_2), 0.67 (m, 6H, Deg γ-CH_3), 0.58 (m, 6H, Deg γ-CH_3).

PyrAc-(Deg)$_2$-*O*-(*p*NO$_2$)Bzl. This compound was prepared from PyrAc-(Deg)$_2$-OH in a 95 : 5 CH_3CN–H_2O mixture as described above for PyrAc-Deg-*O*-(*p*NO$_2$)Bzl. Yield: 50%. Melting point: 166–168 °C (from CH_2Cl_2–PE). TLC R_f1: 0.95; R_f2: 0.95; R_f3: 0.55. IR (KBr): 3340, 1736, 1646, 1520, 1494 cm^{-1}. ^{1}H NMR (200 MHz; $CDCl_3$): δ 8.26 (d, 1H, 1 Pyr CH), 8.21–7.87 (m, 10H, 8 Pyr and 2 Bzl CH), 7.32 (d, 2H, 2 Bzl CH), 6.58 (s, 1H, NH), 6.56 (s, 1H, NH), 5.08 (s, 2H, Bzl CH_2), 4.22 (s, 2H, PyrAc CH_2), 2.35–2.16 (m, 4H, β-CH_2), 1.68–1.50 (m, 4H, β-CH_2), 0.55 (m, 12H, Deg γ-CH_3). MS (ESI-TOF): $[M + H]^+_{calcd}$ 622.299; $[M + H]^+_{exptl}$ 622.288.

PyrAc-(Deg)$_3$-O*t*Bu. This compound was prepared from Tfa-(Deg)$_3$-O*t*Bu as described above for PyrAc-(Deg)$_2$-O*t*Bu. Yield: 83%. Melting point: 188–190 °C (from CH_2Cl_2–PE). TLC R_f1: 0.90; R_f2: 0.95; R_f3: 0.70. IR (KBr): 3336, 1720, 1658, 1491 cm^{-1}. ^{1}H NMR (200 MHz; $CDCl_3$): δ 8.41–7.87 (m, 9H, Pyr CH), 7.21 (s, 1H, NH), 6.89 (s, 1H, NH), 6.76 (s, 1H, NH), 4.29 (s, 2H, PyrAc CH_2), 2.48 (m, 6H, Deg β-CH_2), 1.62 (m, 6H, Deg β-CH_2), 1.47 (s, 9H, O*t*Bu CH_3), 0.78–0.58 (m, 18H, Deg γ-CH_3).

PyrAc-(Deg)$_3$-OH. This compound was prepared from PyrAc-(Deg)$_3$-O*t*Bu as described above for PyrAc-Deg-OH. Yield: 96%. Melting point: 210–212 °C (after repeated washings with Et_2O). TLC R_f1: 0.25; R_f2: 0.95; R_f3: 0.30. ^{1}H NMR (200 MHz; DMSO, d_6): δ 8.19–8.10 (m, 10H, 9 Pyr CH and 1 NH), 7.56 (s, 1H, NH), 7.15 (s, 1H, NH), 4.28 (s, 2H, PyrAc CH_2), 2.20–1.80 (m, 6H, Deg β-CH_2), 1.80–1.65 (m, 6H, Deg β-CH_2), 0.80–0.50 (m, 18H, Deg γ-CH_3).

PyrAc-(Deg)$_3$-*O*-(*p*NO$_2$)Bzl. This compound was prepared from PyrAc-(Deg)$_3$-OH as described above for PyrAc-(Deg)$_2$-*O*-(*p*NO$_2$)Bzl. Yield: 25%. Melting point: 183–184 °C (from CH_2Cl_2–PE). TLC R_f1: 0.95; R_f2: 0.95; R_f3: 0.45. IR (KBr): 3338, 1737, 1648, 1520, 1490 cm^{-1}. ^{1}H NMR (400 MHz; $CDCl_3$): δ 8.34–7.97 (m, 11H, 9 Pyr and 2 Bzl CH), 7.50 (d, 2H, Bzl CH_2), 6.92 (s, 1H, NH^2), 6.62 (s, 1H, NH^3), 6.61 (s, 1H, NH^1), 5.24 (s, 2H, Bzl CH_2), 4.30 (s, 2H, PyrAc CH_2), 2.27 (m, 6H, Deg β-CH_2), 1.86 (m, 2H, Deg β-CH_2), 1.59 (m, 4H, Deg β-CH_2), 0.65 (m, 18H, γ-CH_3). MS (ESI-TOF): $[M + H]^+_{calcd}$ 735.385; $[M + H]^+_{exptl}$ 735.370.

PyrAc-(Deg)$_4$-O*t*Bu. This compound was prepared from Tfa-(Deg)$_4$-O*t*Bu as described above for PyrAc-(Deg)$_2$-O*t*Bu. Yield: 87%. Melting point: 104–106 °C (from EtOAc–PE). TLC R_f1: 0.90; R_f2: 0.95; R_f3: 0.55. IR (KBr): 3332, 1721, 1657, 1490 cm^{-1}. ^{1}H NMR (400 MHz; $CDCl_3$): δ 8.35 (m, 1H, Pyr CH), 8.18–7.93 (m, 8H, 8 Pyr CH), 7.28 (s, 1H, NH), 7.21 (s, 1H, NH), 6.91 (s, 1H, NH), 6.83 (s, 1H, NH), 4.28 (s, 2H, PyrAc CH_2), 2.50 (m, 8H, Deg β-CH_2), 1.64 (m, 8H, Deg β-CH_2), 1.48 (s, 9H, O*t*Bu CH_3), 0.88–0.61 (m, 16H, Deg γ-CH_3).

PyrAc-(Deg)$_4$-*O*-(*p*NO$_2$)Bzl. This compound was prepared from PyrAc-(Deg)$_4$-OH, obtained by acidolysis of PyrAc-(Deg)$_4$-O*t*Bu, as described above for PyrAc-(Deg)$_2$-*O*-(*p*NO$_2$)Bzl. Yield: 52%. Melting point: 180–182 °C (from CH_2Cl_2/PE). TLC R_f1: 0.95; R_f2: 0.95; R_f3: 0.40. IR (KBr): 3411, 3327, 1738, 1672, 1521 cm^{-1}. ^{1}H NMR (400 MHz; $CDCl_3$): δ 8.33 (m, 1H, Pyr CH), 8.15–7.98 (m, 10H, 8 Pyr and 2 Bzl CH), 7.52 (d, 2H, Bzl CH_2), 7.02 (s, 1H, NH^3), 6.82 (s, 1H, NH^2), 6.75 (s, 1H, NH^4), 6.55 (s, 1H, NH^1), 5.26 (s, 2H, Bzl CH_2), 4.30 (s, 2H, PyrAc CH_2), 2.40–2.15 (m, 8H, Deg β-CH_2), 1.91 (m, 2H, Deg β-CH_2), 1.70–1.56 (m, 6H, Deg β-CH_2), 0.77–0.60 (m, 24H, Deg γ-CH_3). MS (ESI-TOF): $[M + H]^+_{calcd}$ 848.471; $[M + H]^+_{exptl}$ 848.447.

PyrAc-(Deg)$_5$-O*t*Bu. This compound was prepared from Tfa-(Deg)$_5$-O*t*Bu as described above for PyrAc-(Deg)$_2$-O*t*Bu. Yield: 89%. Melting point: 207–209 °C (from EtOAc–PE). TLC R_f1: 0.70; R_f2: 0.95; R_f3: 0.40. IR (KBr): 3412, 3319, 1728, 1666, 1527 cm^{-1}. ^{1}H NMR (400 MHz; $CDCl_3$): δ 8.35 (m, 1H, Pyr CH), 8.19–7.95 (m, 8H, 8 Pyr CH), 7.32 (s, 1H, NH), 7.27 (s, 1H, NH), 7.18 (s, 1H, NH), 6.87 (s, 1H, NH), 6.84 (s, 1H, NH), 4.29 (s, 2H, PyrAc CH_2), 2.60–2.33 (m, 10H, Deg β-CH_2), 1.88–1.55 (m, 10H, Deg β-CH_2), 1.48 (s, 9H, O*t*Bu CH_3), 0.85–0.60 (m, 30H, Deg γ-CH_3).

PyrAc-(Deg)$_5$-OH. This compound was prepared from PyrAc-(Deg)$_5$-O*t*Bu as described above for PyrAc-Deg-OH. Yield: 96%. Melting point: 227–229 °C (after repeated washings with Et_2O). TLC R_f1: 0.25; R_f2: 0.95; R_f3: 0.25. ^{1}H NMR (200 MHz; DMSO, d_6): δ 8.59 (s, 1H, NH), 8.53 (m, 1H, Pyr CH), δ 8.27–8.02 (m, 8H, 8 Pyr CH), 7.38 (s, 1H, NH), 6.96 (s, 2H, 2 NH), 6.81 (s, 1H, NH), 4.38 (s, 2H, PyrAc CH_2), 1.80 (m, 10H, Deg β-CH_2), 1.65 (m, 10H, Deg β-CH_2), 0.88–0.54 (m, 30H, Deg γ-CH_3).

PyrAc-(Deg)$_5$-*O*-(*p*NO$_2$)Bzl. This compound was prepared from PyrAc-(Deg)$_5$-OH as described above for PyrAc-(Deg)$_2$-*O*-(*p*NO$_2$)Bzl. Yield: 65%. Melting point: 234–236 °C (from CH_2Cl_2–PE). TLC R_f1: 0.95; R_f2: 0.95; R_f3: 0.35. IR (KBr): 3318, 1737, 1666, 1523 cm^{-1}. ^{1}H NMR (400 MHz; $CDCl_3$): δ 8.36–7.96 (m, 11H, 9 Pyr and 2 Bzl CH), 7.55 (d, 2H, Bzl CH_2), 7.09 (s, 2H, 2 NH), 7.06 (s, 1H, NH), 6.37 (broad s, 1H, NH), 6.17 (broad s, 1H, NH), 5.24 (s, 2H, Bzl CH_2), 4.33 (s, 2H, PyrAc CH_2), 2.20–1.63 (m, 20H, Deg β-CH_2), 0.70–0.58 (m, 30H, Deg γ-CH_3). MS (ESI-TOF): $[M + H]^+_{calcd}$ 961.557; $[M + H]^+_{exptl}$ 961.546.

PyrAc-(Aib)$_5$-O*t*Bu. This compound was obtained from PyrAc–OH and H-(Aib)$_5$-O*t*Bu [the latter prepared in turn from catalytic hydrogenation of Z-(Aib)$_5$-O*t*Bu[32,33] in methanol] as described above for PyrAc-(Deg)$_2$-O*t*Bu. Yield: 26%. Melting point: 296–298 °C (from EtOAc–PE). TLC R_f1: 0.45; R_f2: 0.95; R_f3: 0.20. IR (KBr): 3423, 3322, 1731, 1665, 1525 cm^{-1}. ^{1}H NMR (200 MHz; $CDCl_3$): δ 8.24–7.90 (m, 9H, Pyr CH), 7.29 (s, 1H, NH), 7.28 (s, 1H, NH), 7.12 (s, 1H, NH), 6.00 (s, 1H, NH), 5.81 (s, 1H, NH), 4.27 (s, 2H, PyrAc CH_2), 1.74 (s, 6H, Aib β-CH_3), 1.56 (s, 12H, Aib β-CH_3), 1.50 (s, 12H, Aib β-CH_3), 1.43 (s, 9H, O*t*Bu CH_3).

PyrAc-(Aib)$_5$-OH. This compound was prepared from PyrAc-(Aib)$_5$-O*t*Bu as described above for PyrAc-Deg-OH. Yield: 94%. Melting point: 240–241 °C (after repeated washings with Et_2O). TLC R_f1: 0.25; R_f2: 0.90; R_f3: 0.10. ^{1}H NMR (200 MHz; DMSO, d_6): δ 8.85 (s, 1H, NH), 8.45 (d, 1H, Pyr CH), 8.47–8.00 (m, 9H, 1 NH and 8 Pyr CH), 7.23 (s, 1H, NH), 7.12 (s, 1H, NH), 7.08 (s, 1H, NH), 4.28 (s, 2H, PyrAc CH_2), 1.40 (s, 6H, Aib β-CH_3), 1.25 (s, 6H, Aib β-CH_3), 1.20 (s, 6H, Aib β-CH_3), 1.18 (s, 6H, Aib β-CH_3), 0.64 (s, 6H, Aib β-CH_3).

PyrAc-(Aib)$_5$-*O*-(*p*NO$_2$)Bzl. This compound was obtained from PyrAc-(Aib)$_5$-OH as described above for PyrAc-(Deg)$_2$-*O*-(*p*NO$_2$)Bzl. Yield: 87%. Melting point: 234–236 °C (from EtOAc–PE). TLC R_f1: 0.75; R_f2: 0.95; R_f3: 0.25. IR (KBr): 3318, 1740, 1663, 1523 cm^{-1}. ^{1}H NMR (400 MHz; $CDCl_3$): δ 8.35–7.98 (m, 11H, 9 Pyr and 2 Bzl CH), 7.48 (s, 1H, NH), 7.39 (d, 2H, 2 Bzl CH), 7.30 (s, 1H, NH), 7.12 (s, 1H, NH), 6.47 (s, 1H, NH), 5.81 (s, 1H, NH), 5.16 (s, 2H, Bzl CH_2), 4.25 (s, 2H, PyrAc CH_2), 1.50 (s, 6H, Aib β-CH_3), 1.40 (s, 6H, Aib β-CH_3), 1.30 (s, 6H, Aib β-CH_3), 1.28 (s, 6H, Aib β-CH_3), 0.92 (s, 6H, Aib β-CH_3). MS (ESI-TOF): $[M + H]^+_{calcd}$ 821.397; $[M + H]^+_{exptl}$ 821.385.

Tfa-(Deg)$_4$-*O*-(*p*NO$_2$)Bzl. This compound was obtained from Tfa-(Deg)$_4$-O*t*Bu *via* formation (without isolation) of the intermediate Tfa-(Deg)$_4$-OH. The procedures for the two steps are those described above for PyrAc-Deg-OH and PyrAc-(Deg)$_2$-*O*-(*p*NO$_2$)Bzl, respectively. Yield: 72%. Melting point: 185–187 °C (from CH_2Cl_2–PE). TLC R_f1: 0.95; R_f2: 0.95; R_f3: 0.55. IR (KBr): 3346, 1726, 1655, 1523, 1492 cm^{-1}. ^{1}H NMR (400 MHz; $CDCl_3$): δ 8.25 (d, 2H, 2 Bzl CH), 7.99 (s, 1H, NH), 7.54 (d, 2H, 2 Bzl CH), 7.39 (s, 1H, NH), 7.28 (s, 1H, NH), 6.59 (s, 1H, NH), 5.37 (s, 2H, Bzl CH_2), 2.73–2.38 (m, 8H, Deg β-CH_2), 1.90–1.63 (m, 8H, Deg β-CH_2), 0.89–0.68 (m, 24H, Deg γ-CH_3). MS (ESI-TOF): $[M + H]^+_{calcd}$ 702.378; $[M + H]^+_{exptl}$ 702.349.

Ac-*O*-(*p*NO$_2$)Bzl. This compound was prepared from acetic acid (AcOH) as described above for PyrAc-(Deg)$_2$-*O*-(*p*NO$_2$)Bzl. Yield: 71%. Melting point: 74–76 °C (from CH_2Cl_2–PE). TLC R_f1: 0.95; R_f2: 0.95; R_f3: 0.85. IR (KBr): 1738, 1655, 1520 cm^{-1}. ^{1}H NMR (200 MHz; $CDCl_3$): δ 8.13 (d, 2H, 2 Bzl CH), 7.19 (d, 2H, 2 Bzl CH), 5.13 (s, 2H, Bzl CH_2), 2.08 (s, 3H, Ac CH_3).

FT-IR absorption

The FT-IR absorption spectra were recorded at 293 K using a Perkin Elmer model 1720X FTIR spectrophotometer, nitrogen flushed, equipped with a sample shuttle device, at 2 cm^{-1} nominal resolution, averaging 100 scans. Cells with path lengths of 0.1, 1.0, and 10 mm (with CaF_2 windows) were used. Spectrograde deuterated chloroform (99.8%, d) was purchased from Aldrich (Milwaukee, WI). Solvent (baseline) spectra were recorded under the same conditions.

Nuclear magnetic resonance

The ^{1}H NMR spectra were recorded with Bruker AC 200 and AM 400 spectrometers. Measurements were carried out in $CDCl_3$ (99.96%, d; Aldrich) and deuterated DMSO (99.96%, d_6; Acros Organics) with tetramethylsilane as the internal standard. Splitting patterns are abbreviated as follows: (s) singlet, (d) doublet, (t) triplet, (q) quartet, (qd) quartet of doublets, (m) multiplet. The 2D-NMR experiments were performed with a Bruker AVANCE DRX-400 spectrometer, operating at 400 MHz, equipped with a 5 mm probe BBI-Z grad. Processing and evaluation of the experimental data were carried out using the programs TOPSPIN 1.3 and SPARKY.[47] The DQF-COSY[48] spectra were acquired in magnitude mode, while CLEAN-TOCSY[49,50] (spin lock period: 70 ms) and NOESY spectra were recorded in the phase-sensitive mode. All homonuclear 2D spectra were acquired by collecting 400–512 experiments of 64–128 scans each, with a relaxation delay of 1.0–1.2 s, and 2 K data points. The spectral width was 11 ppm in each dimension.

Fluorescence

Steady-state fluorescence spectra on the PyrAc-containing peptides were recorded with a Jobin Ivon Fluoromax-2 (Longjumeau, France) spectrofluorimeter. Cells with path length of 1 cm were used. Spectrograde MeOH was purchased from Fluka (Büchs, Switzerland).

X-Ray diffraction

Single crystals of PyrAc-(Deg)$_2$-*O*-(*p*NO$_2$)Bzl and PyrAc-(Deg)$_5$-*O*-(*p*NO$_2$)Bzl were grown by slow evaporation from methanol–dichloromethane mixtures, while those of PyrAc-(Aib)$_5$-O*t*Bu by slow evaporation from methanol. X-ray diffraction data were collected with an Agilent Gemini E four-circle kappa diffractometer equipped with a 92 mm EOS CCD detector, using graphite monochromated Cu Kα radiation (λ = 1.54178 Å). The structures were solved by direct methods of the SIR 2002 program,[51] and refined by full-matrix least-squares procedures on F^2, using all data, by application of the SHELXL-97 program,[52] with all non-H atoms anisotropic. H-atoms were calculated at idealized positions and refined using a riding model. Crystal structure data have been deposited at the Cambridge Crystallographic Data Centre‡, and allocated the deposition numbers CCDC 846155, CCDC 846156, and CCDC 846157 for PyrAc-(Deg)$_2$-*O*-(*p*NO$_2$)Bzl, PyrAc-(Deg)$_5$-*O*-(*p*NO$_2$)Bzl, and PyrAc-(Aib)$_5$-O*t*Bu, respectively.

Crystal data for PyrAc-(Deg)$_2$-*O*-(*p*NO$_2$)Bzl: $C_{37}H_{39}N_3O_6$, M = 621.71, monoclinic, space group $P2_1/n$, a = 10.68181(10) Å, b = 11.93226(15) Å, c = 25.6913(3) Å, β = 93.4477(9)°; V = 3268.64(6) Å^3, Z = 4; ρ_{calcd} = 1.263 Mg m^{-3}, μ = 0.697 mm^{-1}, 43 609 reflections measured, 6306 independent reflections (R_{int} = 0.0562), θ_{max} = 71.44°, T = 295(2) K. The N-terminal PyrAc group shows librational disorder. It was refined on two sets of positions (atoms C01 to C17 and C01′ to C17′, respectively) with refined occupancies of 0.674(16) and 0.326(16). Restraints were applied to the bond distances, planarity, and anisotropic displacement parameters of the disordered parts. The final R_1 values were 0.0539 [$I > 2\sigma(I)$] and 0.0591 (all data). The final w$R(F^2)$ values were 0.1549 [$I > 2\sigma(I)$] and 0.1621 (all data). Data/restraints/parameters 6306/188/570. Goodness-of-fit on F^2 = 1.032. The largest difference peak and hole were 0.276 and −0.247 e Å^{-3}, respectively.

Crystal data for PyrAc-(Deg)$_5$-*O*-(*p*NO$_2$)Bzl: $C_{55}H_{72}N_6O_9$, M = 961.19, monoclinic, space group $P2_1$, a = 10.0556(2) Å, b = 23.1736(5) Å, c = 11.9038(2) Å, β = 98.010(2)°; V = 2746.81(9) Å^3, Z = 2; ρ_{calcd} = 1.162 Mg m^{-3}, μ = 0.638 mm^{-1}, 38 894 reflections measured, 10 511 independent reflections (R_{int} = 0.0329), θ_{max} = 72.39°, T = 293(2) K. Although lacking chiral carbon atoms, the molecule crystallizes in a chiral space group. The chosen enantiomorph is that giving the lowest value for the

Flack parameter [0.0(2)]. Restraints were applied to the anisotropic displacement parameters of a number of atoms belonging to the PyrAc moiety, the C^{γ} atoms of the Deg residues, and the O atoms of the C-terminal nitro group. The final R_1 values were 0.0638 [$I > 2\sigma(I)$] and 0.0705 (all data). Data/restraints/parameters 10 511/91/631. The goodness of fit on F^2 was 1.032. The largest difference peak and hole were 0.661 and −0.206 e Å $^{-3}$, respectively.

Crystal data for PyrAc-(Aib)$_5$-O*t*Bu: $C_{42}H_{55}N_5O_7$, M = 741.91, triclinic, space group $P\bar{1}$, a = 11.5910(8) Å, b = 12.4620 (8) Å, c = 15.4573(12) Å, α = 97.958(1)°, β = 107.430(1)°, γ = 91.224(1)°; V = 2105.1(3) Å^3, Z = 2; ρ_{calcd} = 1.170 Mg m^{-3}, μ = 0.647 mm^{-1}, 37 968 reflections measured, 8448 independent reflections (R_{int} = 0.0328), θ_{max} = 73.34°, T = 293(2) K. Restraints were applied to the anisotropic displacement parameters of a number of atoms belonging to the PyrAc moiety and the C-terminal *t*Bu group. The final R_1 values were 0.0537 [$I > 2\sigma(I)$] and 0.0559 (all data). The final w$R(F^2)$ values were 0.1598 [$I > 2\sigma(I)$] and 0.1638 (all data). Data/restraints/parameters 8448/66/487. The goodness of fit on F^2 was 1.031. The largest difference peak and hole were 0.266 and −0.237 e Å^{-3}, respectively.

Acknowledgements

M. C. is grateful to Prof. A. Dolmella (Department of Pharmaceutical Sciences, University of Padova) for granting access to the Gemini diffractometer and for his help with X-ray data collection and processing. Financial support for the acquisition of the Agilent Gemini diffractometer was provided by the University of Padova through the 2008 "Scientific Equipment for Research" initiative.

Notes and references

1 G. R. Marshall in *Intra-Science Chemistry Report*, ed. N. Kharasch, Gordon and Breach, New York, 1971, Vol. 5, pp. 305–316.
2 I. L. Karle and P. Balaram, *Biochemistry*, 1990, **29**, 6747–6756.
3 C. Toniolo, M. Crisma, F. Formaggio and C. Peggion, *Biopolymers*, 2001, **60**, 396–419.
4 V. Barone, F. Lelj, A. Bavoso, B. Di Blasio, P. Grimaldi, V. Pavone and C. Pedone, *Biopolymers*, 1985, **24**, 1759–1767.
5 E. Benedetti, V. Barone, A. Bavoso, B. Di Blasio, F. Lelj, V. Pavone, C. Pedone, G. M. Bonora, C. Toniolo, M. T. Leplawy, K. Kaczmarek and A. Redlinski, *Biopolymers*, 1988, **27**, 357–371.
6 C. Toniolo, G. M. Bonora, A. Bavoso, E. Benedetti, B. Di Blasio, V. Pavone, C. Pedone, V. Barone, F. Lelj, M. T. Leplawy, K. Kaczmarek and A. Redlinski, *Biopolymers*, 1988, **27**, 373–379.
7 C. Toniolo and E. Benedetti, *Macromolecules*, 1991, **24**, 4004–4009.
8 C. Toniolo and E. Benedetti, in *Molecular Conformation and Biological Interactions*, ed. P. Balaram and S. Ramaseshan, Indian Academy of Sciences, Bangalore, India, 1991, pp. 511–521.
9 E. Benedetti, B. Di Blasio, V. Pavone, C. Pedone, C. Toniolo and M. Crisma, *Biopolymers*, 1992, **32**, 453–456.
10 K. Ramnarayan, M. F. Chan, V. N. Balaji, S. Profeta, Jr. and S. N. Rao, *Int. J. Pept. Protein Res.*, 1995, **45**, 366–376.
11 M. Cirilli, V. M. Coiro, A. Di Nola and F. Mazza, *Biopolymers*, 1998, **46**, 239–244.
12 M. Tanaka, N. Imawaka, M. Kurihara and H. Suemune, *Helv. Chim. Acta*, 1999, **82**, 494–510.
13 M. Kurihara, M. Tanaka, M. Oba, H. Suemune and N. Miyata, in *Peptides 2000*, ed. J. Martinez and J.-A. Fehrentz, EDK, Paris, France, 2001, pp. 427–428.
14 M. A. C. Preto, A. Melo, S. P. G. Costa, H. L. S. Maia and M. J. Ramos, *J. Phys. Chem. B*, 2003, **107**, 14556–14562.
15 C. Toniolo, M. Crisma, F. Formaggio, C. Peggion, Q. B. Broxterman and B. Kaptein, *Biopolymers*, 2004, **76**, 162–176.
16 M. Crisma, F. Formaggio, A. Moretto and C. Toniolo, *Biopolymers*, 2006, **84**, 3–12.
17 M. Crisma, E. Andreetto, M. De Zotti, A. Moretto, C. Peggion, F. Formaggio and C. Toniolo, *J. Pept. Sci.*, 2007, **13**, 190–205.
18 J. Torras, D. Zanuy, M. Crisma, C. Toniolo, O. Betran and C. Aleman, *Biopolymers*, 2008, **90**, 695–706.
19 A. Moretto, M. De Zotti, M. Crisma, F. Formaggio and C. Toniolo, *Int. J. Pept. Res. Ther.*, 2008, **14**, 307–314.
20 C. Toniolo and E. Benedetti, *Trends Biochem. Sci.*, 1991, **16**, 350–353.
21 F. Formaggio, M. Crisma, C. Peggion, A. Moretto, M. Venanzi and C. Toniolo, *Eur. J. Org. Chem.*, 2012, 167–174.
22 C. Peggion, M. Crisma, C. Toniolo and F. Formaggio, *Tetrahedron*, 2012, in press.
23 M. T. Cung, M. Marraud and J. Néel, *Ann. Chim. (Paris)*, 1972, **7**, 183–209.
24 C. Toniolo, *Crit. Rev. Biochem. Mol. Biol.*, 1980, **9**, 1–44.
25 E. Prasad and K. R. Gopidas, *J. Am. Chem. Soc.*, 2000, **122**, 3191–3196.
26 M. Sisido, S. Hoshino, H. Kusano, M. Kuragaki, M. Makino, H. Sasaki, T. A. Smith and J. P. Ghiggino, *J. Phys. Chem. B*, 2001, **105**, 10407–10415.
27 M. T. Leplawy, K. Kaczmarek and A. Redlinski, in *Peptides: Chemistry and Biology*, ed. G. R. Marshall, ESCOM, Leiden, The Netherlands, 1988, pp. 239–241.
28 Z. Kaminski, M. T. Leplawy, A. Olma and A. Redlinski, in *Peptides 1980*, ed. K. Brunfeldt, Scriptor, Copenhagen, Denmark, 1981, pp. 201–206.
29 W. J. McGahren and M. Goodman, *Tetrahedron*, 1967, **23**, 2017–2030.
30 L. A. Carpino, *J. Am. Chem. Soc.*, 1993, **115**, 4397–4398.
31 L. A. Carpino, A. El-Faham, C. A. Minor and F. Albericio, *Chem. Commun.*, 1994, 201–203.
32 D. S. Jones, G. W. Kenner, J. Preston and R. C. Sheppard, *J. Chem. Soc.*, 1965, 6227–6239.
33 E. Benedetti, A. Bavoso, B. Di Blasio, V. Pavone, C. Pedone, M. Crisma, G. M. Bonora and C. Toniolo, *J. Am. Chem. Soc.*, 1982, **104**, 2437–2444.
34 W. G. Touw and G. Vriend, *Acta Crystallogr., Sect. D: Biol. Crystallogr.*, 2010, **66**, 1341–1350.
35 L. Pasteur, *C. R. Acad. Sci. (Paris)*, 1848, **26**, 35.
36 L. Pérez-García and D. B. Amabilino, *Chem. Soc. Rev.*, 2002, **31**, 342–356.
37 H. D. Flack, *Acta Crystallogr., Sect. A: Found. Crystallogr.*, 1983, **39**, 876–881.
38 H. D. Flack and G. Bernardinelli, *J. Appl. Crystallogr.*, 2000, **33**, 1143–1148.
39 C. H. Görbitz, *Acta Crystallogr., Sect. B: Struct. Sci.*, 1989, **45**, 390–395.
40 C. Toniolo, G. M. Bonora, V. Barone, A. Bavoso, E. Benedetti, B. Di Blasio, P. Grimaldi, F. Lelj, V. Pavone and C. Pedone, *Macromolecules*, 1985, **18**, 895–902.
41 D. F. Kennedy, M. Crisma, C. Toniolo and D. Chapman, *Biochemistry*, 1991, **30**, 6541–6548.
42 K. D. Kopple, M. Ohnishi and A. Go, *J. Am. Chem. Soc.*, 1969, **91**, 4264–4272.
43 *Dimethyl Sulphoxide*, ed. D. Martin and H. G. Hauthal, van Rostrand-Reinhold, Wokingham, UK, 1975.
44 V. Moretto, M. Crisma, G. M. Bonora, C. Toniolo, H. Balaram and P. Balaram, *Macromolecules*, 1989, **22**, 2939–2944.
45 F. Formaggio, Q. B. Broxterman and C. Toniolo, in *Houben-Weyl: Methods of Organic Chemistry*, ed. M. Goodman, A. Felix, L. Moroder and C. Toniolo, Thieme, Stuttgart, Germany, 2003, pp. 292–310.
46 S. M. Holl, G. R. Marshall, D. D. Beusen, K. Kociolak, A. S. Redlinski, M. T. Leplawy, R. A. McKay, S. Vega and J. Schaefer, *J. Am. Chem. Soc.*, 1992, **114**, 4830–4833.
47 T. D. Goddard and D. G. Kneller, SPARKY 3, University of California, San Francisco, CA.
48 M. Rance, O. W. Sørensen, G. Bodenhausen, G. Wagner, R. R. Ernst and K. Wüthrich, *Biochem. Biophys. Res. Commun.*, 1983, **117**, 479–485.
49 A. Bax and D. G. Davis, *J. Magn. Reson.*, 1985, **65**, 355–360.
50 C. Griesinger, G. Otting, K. Wüthrich and R. R. Ernst, *J. Am. Chem. Soc.*, 1988, **110**, 7870–7872.
51 M. C. Burla, M. Camalli, B. Carrozzini, G. L. Cascarano, C. Giacovazzo, G. Polidori and R. Spagna, *J. Appl. Crystallogr.*, 2003, **36**, 1103.
52 G. M. Sheldrick, *Acta Crystallogr., Sect. A: Found. Crystallogr.*, 2008, **64**, 112–122.